JEE Journal of Ecological Engineering

Journal of Ecological Engineering 2023, 24(11), 135–147
https://doi.org/10.12911/22998993/171543
ISSN 2299–8993, License CC-BY 4.0

Received: 2023.07.03
Accepted: 2023.08.31
Published: 2023.09.15

Extraction of the Spatial and Temporal Surface Water Bodies Using High Resolution Remote Sensing Technology at Cardiff City, United Kingdom

Hayder H. Kareem[1*], Muammar H. Attaee[2], Zainab Ali Omran[3]

[1] Structures and Water Resources Engineering Department, Faculty of Engineering, University of Kufa, Al-Najaf, Iraq

[2] Department of Civil Engineering, College of Engineering, University of Misan, Misan, Amarah 62001, Iraq

[3] Department of Civil Engineering, Faculty of Engineering, University of Babylon, Babil, Iraq

[*] Corresponding author's e-mail: hayderh.alshaibani@uokufa.edu.iq

ABSTRACT

Since surface water is such a vital component to ecosystem health and human well-being, knowing where it can be found is of paramount importance. Moderate and low-resolution satellite photos are widely used for this purpose because to their practicality in large-scale implementation. However, very high-resolution (VHR) satellite pictures are required for the detection and analysis of more intricate surface water features and small water bodies. Extraction of water from VHR pictures on a wide scale necessitates efficient and reliable technologies. Cardiff City in Wales, United Kingdom is the area under investigation for the Enhanced Water Index (EWI) which will through this index can detect the surface water bodies (SWBs). The Multispectral Scanner (MSS), Thematic Mapper (TM), Enhanced Thematic Mapper Plus ETM+, and Operational Land Imager OLI Landsat images have been analyzed to extract SWBs over the years 1974, 1984, 1994, 2004, 2014, and 2023. Results shows that the years 1974, 1994, and 2014 have less SWBs regions compared to the years 1984, 2004, and 2023. Regions suffer from dry were larger than those contain water in the years 1974, 1994, and 2014, while in the years 1984, 2004, and 2023, SWBs were very large, leaving behind small areas that suffered from drought. It can expect from this study that the return period of dryness or wetness may happen every 20 years. This research can be used as a reference when developing new methods for extracting water body information from VHR photos, and it can be used to the mapping of water bodies in other broad regions.

Keywords: surface water bodies, EWI, landsat images, spatial and temporal detection, GIS, Cardiff City, United Kingdom.

INTRODUCTION

Water is essential for all forms of life. Water is essential not only to the continued existence of humans and other animals, but also to the progress of civilization and the growth of human society. Rivers, lakes, glaciers, and swamps are all types of surface water (SW). It is the primary component of the world's freshwater resources, and it plays a crucial function in preserving the ecological stability of river basins and satisfying human needs for energy, water, irrigation, manufacturing, and other uses. Interestingly, the effect of climate isolation in addition to the humanity activities have added an impact on surface water bodies (SWB) and this can be reflected and characterized by variations in the area of surface water. Research into flood and drought disasters, water resource monitoring, and water resource management all benefit greatly from being able to quickly and reliably extract SWB information and grasp the geographical distribution of water over an area (Garrido-Rubio et al., 2020; Papa et al., 2022). Both natural and human-caused factors pose risks to the availability of surface water in arid and semiarid regions. If we are to effectively manage and address the decline of water quantity and quality, we must first map the distribution of SWBs (Malahlela, 2016). Most water was gleaned from the ground prior to the use of remote sensing technology for mapping water resources. There are obstacles to satisfying the spatial and temporal requirements because of the manual method's low precision, vast heavy workload, high expense, and ineffective macro control of the applied processes, real-time, and impactful monitoring. However, remote sensing technology has advantages including low cost, dynamic monitoring, and data collection on a large scale. Water data extracted from remote sensing images can help us better understand the location, health, and trajectory of basins' water bodies, as well as provide essential baseline information for flood observation and water resource protection and conservation (Domeneghetti et al., 2019; Aznarez et al., 2021; Bretreger et al., 2021).

There are currently a plethora of methods available for gleaning water data from satellite photos. Single band method (Yang and Ruan, 2010; Lu et al., 2021), spectral relationship method [Zhang et al., 2018; Aznarez et al., 2021), picture classification method (Vinayaraj et al., 2018), and water index method (McFeeters, 1996) are some of the broad categories into which these techniques fall. The water index technique is one of the most extensively utilized indices in the scientific community. The water remote sensing index-based technology is the most popular choice among the several available methods for extracting data from water satellite images. The water remote sensing index is now practically indispensable in mapping the distribution of SW on a global and regional scale. The first global high-resolution satellite maps of land-based bodies of water (Yamazaki et al., 2015) was conducted by a select group of researchers using the normalized difference water index (NDWI) and the modified NDWI water index (MNDWI). The global distribution range and area of rivers can be determined using MNDWI as a key algorithm (Allen and Pavelsky, 2018). Complex terrains including inland waterways, wetlands, delta regions, coastal areas, dry, arid, and semiarid regions, and more (Müller et al., 2016; Zou et al., 2016; Allen and Pavelsky, 2018; Chen and Mueller, 2018; Colditz et al., 2018; Ogilvie et al., 2018; Acharya et al., 2019) all make use of water indices thanks to their construction and improvement, allowing for comparison of the consequences of surface-water-extraction techniques in various places. The water extraction investigations conducted so far have yielded promising findings for the research region. The advantages of various water indices for obtaining surface water data vary. Using typical ground object sample locations in the research region and the spectral dissimilarity in information, new water indices may be constructed. Their levels of extraction accuracy and area-specific differentiation effect are often quite high.

Normalized difference water index (NDWI) is one of the most prominent water index algorithms since it reduces the weight of non-hydrological aspects like plant and soil composition. Despite the fact that it conveys a great deal of interfering data in urban water extraction (McFeeters, 1996), it's a common method for draining water from huge bodies of water.. On the back of the NDWI method, we present the modified normalized difference water index (MNDWI) that makes use of Landsat TM short wave infrared rather than near-infrared imagery. While MNDWI can reduce the effect of soil and structures, it is quite effective at eliminating building shadows in metropolitan areas. Wetlands in eastern Australia are extracted using the water index WI2006, which leverages the natural pairings of each band of Landsat 7 ETM+ images to address for the coefficient of reflection and interaction (Danaher and Collett, 2006). Landsat photos are processed to extract information on water systems from the green light band, the near-infrared band, and the mid-infrared band. This is known as the enhanced water index (EWI). With this indicator, researchers can filter out the effects of the weather (Yan et al., 2007).

It is commonly accepted that different types of water respond differently to extraction depending on the water index used. Therefore, the Enhanced Water Index (EWI) will be detected in the study region to obtain water body information. In this study, we use remote sensing data from the Landsat TM, ETM+, and OLI series obtained in 1974, 1984, 1994, 2004, 2014, and 2023 to identify and map Cardiff City's water features, as Cardiff City in Wales, United Kingdom (UK) is considered as the study area in this research. The findings of this study have considerable implications for the water resource management based on science in the area under investigation, and can assist researchers gain a better knowledge in light of the persistent and ever-shifting surface-water fluctuations in the region.

RESEARCH REGION

Cardiff is both the nation's administrative center and largest metropolis. Cardiff, which in 2021 had a population of 362,310 is the eleventh-largest city in the UK and the core area of which is formally known as the City of Cardiff. Cardiff is the town of Glamorgan, the ancient county, and South Glamorgan, the modern county, in Wales's south-east. It's one of the major cities in Europe, hence it's part of the Euro-cities group. When coal mining began in the area, the town grew rapidly because of its strategic location as a port for the commodity. It was recognized as a city in 1905 and became the capital of Wales in 1955. Cardiff Built-up area extends beyond the county limits to encompass urban centers like Dinas Powys and Penarth. Cardiff serves as the seat of government for Wales and is also its primary commercial hub. The population of the unitary authority region was estimated to be 362,400 as of the 2021 census. In 2011, the metropolitan region as a whole had a population of 479 thousand people (UK Census, 2011). In 2011, National Geographic magazine listed it as the sixth best alternative travel destination in the world with 21.3 million people in 2017, it is Wales' most visited attraction (Cardiff Boasts Record Visitor Numbers During, 2017).

Cardiff's hills to the east, north, and west provide a comparatively flat central area. Its closeness to South Wales Valleys played a significant role in the city's rise to prominence as the world's largest coal port. Garth Hill, at an elevation of 307 meters (1,007 feet), is the highest point in the municipality's jurisdiction. Cardiff was constructed over previously drained marshland resting atop Triassic rocks. Cardiff and the Vale of Glamorgan are separated by the natural boundary that runs across the reclaimed marshes from Chepstow to the Ely Estuary. The typical shallow and low-lying Triassic landscapes of this region are in keeping with the level topography of downtown Cardiff (Radley et al., 2008). Traditional Triassic marl, sandstone, and conglomerate are often employed in Cardiff's construction. The coastal marl in the area around Penarth is particularly purple, as are many of the other Triassic rocks. The "Radyr Stone" used around Cardiff is a freestone that originates in the Radyr region and is one of the Triassic rocks mined there. The Brecon Beacons' Devonian sandstones (the Old Red Sandstone) have been utilized in construction in Cardiff. The most well-known examples of Portland stone architecture in the city can be seen in the structures in Cathays Park, the city's civic center. The yellow-grey "Sutton Stone" is one of the rarer types of the Vale of Glamorgan's Liassic limestone, which is commonly utilized as a building stone in Cardiff (Iowerth, 1998). Geographical features that surround Cardiff include the South Wales Valleys to the north, the South Wales Coast to the east, the Severn Estuary to the south, and the Bristol Channel to the west. The city's central area is traversed by the River Taff, which, along with the River Ely, eventually empties into Cardiff Bay.

The Rhymney, a third river, cuts through the city's eastern neighborhoods and empties into the Severn Estuary.

Cardiff, located in the north temperate zone, experiences a marine climate characterized by mild weather that is frequently gloomy, damp, and windy. The summers are typically hot and sunny, with highs averaging between 19 and 22 °C. The winters are typically wet, but extreme precipitation and freezing temperatures are unusual. The average yearly daytime temperature is 14 °C, thus spring and fall both feel about the same. The length of a rain shower varies by season, but often is shorter in the summer (Weather at Cardiff Airport, 2009). Since it is higher and further inland, the northern half of the county experiences more rain and cooler temperatures than the city proper. The hottest month (July) and the coldest (February) temperatures in Cardiff typically reach 21.5 °C and 2.1 °C, respectively. July averages 19.1 °C and February averages 1.1 °C in Wales. Average annual sunshine in Cardiff is 1,518 hours, compared to 1,388.7 hours across Wales. Average sunshine hours in Cardiff are 203.4 in July (Wales average is 183.3) and 44.6 in December (Wales average is 38.5). Rainfall in Cardiff is lower than the Welsh average. The average yearly precipitation is 1,151.9 mm and it rains on 146 days a year. From October to January, the wettest month is December, with an average rainfall of 125.3 mm and the driest months are April and June, with an typical monthly precipitation between 65 and 75 mm Met Office: averages 1971–2000, 2009). Figures 1 and 2 display the elevation levels based on the downloaded Digital Elevation Model (DEM) of Cardiff City with a three-dimensional representation of the land surface, respectively.

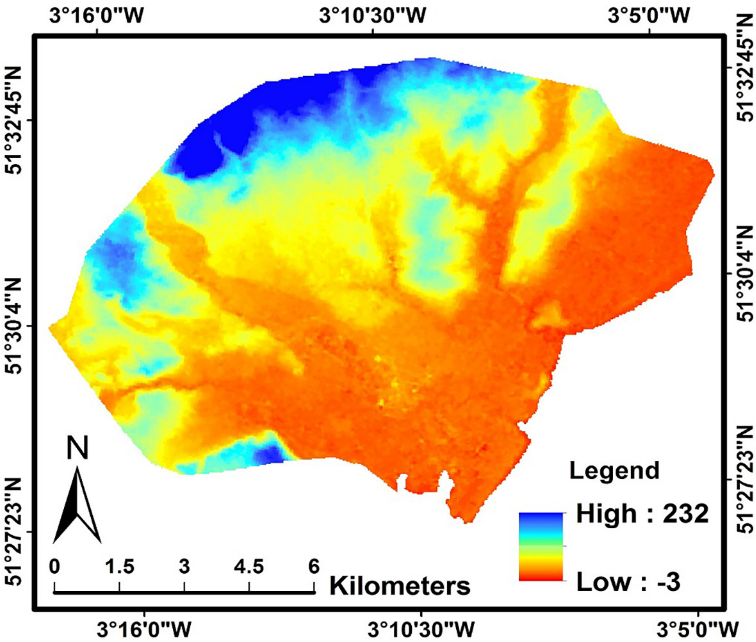

Figure 1. Downloaded digital elevation model (DEM) of Cardiff City

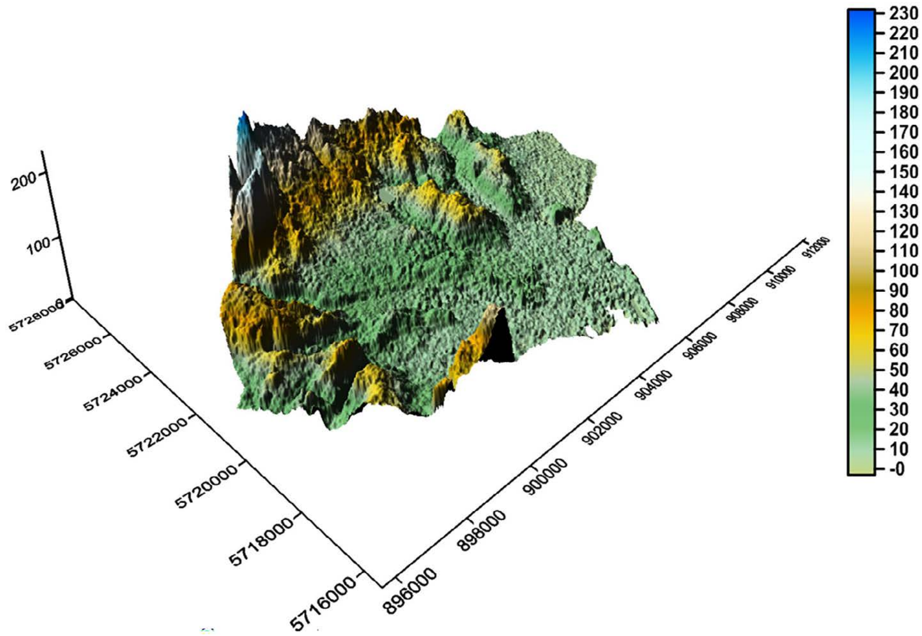

Figure 2. 3-Dimensional view of land surface elevations of Cardiff City

METHODOLOGY

Wet- and dry-season Landsat satellite images for 1974, 1984, 1994, 2004, 2014, and 2023 were downloaded from the US Geological Survey's Earth Explorer website (http://earthexplorer.usgs.gov/). If you want to track changes in land use circumstances, you'll need data from at least two time points to draw meaningful conclusions (Alam et al., 2020). Because of their wide availability and reasonable resolution for the extent of the study area and our computational resources, we settled on Landsat photos. We chose these years based on information we have about the catchment's past. We expected that accelerated advancements in areas such as agricultural reform and dramatic climate changes had environmental repercussions that affected the dissection of rainfall into its component parts. Since the climatic relief caused by the major changes was not clearly visible in the impact on land areas and watersheds prior to 1974, we assumed that year to be the baseline.

The succeeding 10-year intervals were thus used to better reflect the intensity with which land use and land cover in the watershed have changed as a result of both natural and human activity. Notably, despite prompt actions, changes in land cover are frequently a slow process. The properties of the Landsat pictures used in the analysis are displayed in Table 1. Best times to collect data were determined by thinking about things like image quality, scene availability and coverage (Path/row), and cloud cover (,1%). As a result, photos from the wet/dry-season-ending years were selected to depict the phenological maturity of the studied plant.

After examining the various water body indices that have been developed over the past two decades, we find that the EWI best fits our expectations. This is because it is the most widely used water index, and numerous experiments conducted by various researchers have confirmed the EWI's efficacy in extracting water bodies. However, the research by EWI's developers demonstrates that the technology can identify bodies of water from ambient noise in a wide range of geographical settings and climate conditions. We settled on EWI as the method to employ for obtaining water features (Feyisa et al., 2014; Gao et al., 2021) in the study region. Here is an explanation of the formula used to determine the EWI:

$$EWI = \frac{\rho Green - \rho NIR - \rho MIR}{\rho Green + \rho NIR + \rho MIR} \tag{1}$$

where: ρ represents the band reflectance value where band reflectance subscripts correspond to the relevant bands in various remote sensing photographs.

LANDSAT 8 OLI IMAGE PROCESSING

There is no doubt that time-series data is superior for tracking variations in the natural world. A major trend in the future is the use of remote sensing platforms for large-scale data processing and analysis. Compared to simple categorization, the time-aware mapping method is clearly superior. The accuracy of biomass assessment in water bodies has been shown to improve with the use of multi-seasonal images. It has also been noted that multi-temporal data is useful for estimating successional processes. Spectrum products from the same sensor are more spatially consistent than multi-source picture products when used for time-series monitoring remote sensing mapping. Scholars have found that the long acquisition time, vast amounts of stored data, and high spatial resolution of Landsat satellite photos (Tariq et al., 2021) make them particularly useful. It is difficult to create time series remote sensing products from satellite images because of gaps in the data and poor data quality. Possibilities for the time-series products arise from the pixel classification, which makes use of optimal observational frequency for generating images. Synthetic images at the pixel level can be created from a long-sequence Landsat image set to create a time-series period (Parente et al., 2019; Somasundaram et al., 2020).

Accurate forecasts are made possible by synthesizing the benefits of land use change attributes at a single site across many time phases, which in turn yields cloudless, smooth, and continuous synthetic images. Recent high variability in surface water has been measured by researchers using "per pixel frequency". This strategy works particularly well in areas where cloud-free data is scarce. Precision pixel size estimation properties is crucial to temporal pattern analysis because of the regional hydrodynamic complexity. There has

Table 1. Landsat data used to extract EWI of the surface water bodies of Cardiff City

Satellite	Sensor	Year	Spatial resolution (m)	Cloud cover	Wavelength of used bands (nm)
Landsat-3	MSS	1974	30	0%	B4 = 0.5 – 0.6 B6 =0.7 – 0.8 B7 = 0.8 – 1.1
Landsat-5	TM	1984	30	0%	B2= 0.52 – 0.60 B4 = 0.76 – 0.90 B5 = 1.55 – 1.75
Landsat-5	TM	1994	30	0%	
Landsat-5	TM	2004	30	0%	
Landsat-7	ETM+	2014	30	0%	
Landsat-8	OLI	2023	30	0%	B3 = 0.533 – 0.590 B5 = 0.851 – 0.879 B6 = 1.556 – 1.651

to be some theoretical and practical discussion about calculating pixel frequency. This research advances the theory of pixel frequency computation and examines the frequency statistical approach of interannual "water" and "non-water" categorization. Most vulnerable to climate change are ecosystems dependent on surface water. Wetland ecosystems are particularly vulnerable to climate change because their very makeup, structure, distribution, and function are all intertwined with weather patterns. The study of seasonal water body variations requires automatic mapping of time series in particular, and picture extraction for small bodies of water.

In addition to the information shown above, models for both WB extraction and mapping frequencies will be built using Landsat 3–8 surface reflectance data, allowing for highly automated time-series mapping of SW in the city of Cardiff. This will allow us to examine the links between surface water and extreme climate using all available climate data.

Landsat data gives us a time frame of 1974 to 2023. Bands within the images are processed to filter out traffic and eliminate clouds. Images captured by the 'B4', 'B6', and 'B7' bands of Landsat-3 MSS, the 'B2', 'B4', and 'B5' bands of Landsat-5 TM and Landsat-7 ETM+, and the 'B3', 'B5', and 'B6' bands of Landsat 8 OLI are all calibrated to the Green, NIR, and MIR. These bands serve as a foundation for selecting sample points and one of the pillars upon which the effect of extracting water from the surface is based. For each Landsat series, the GIS Composite Bands function is used is as a tool for calculating the average reflectance of diverse ground objects throughout a given sample, which can be used to create a spectral characteristic of typical ground objects in Cardiff City, which serves as a reflection of the accuracy of the sample point selection. The Composite Bands results for each Landsat's Green, NIR, and MIN bands in 1974, 1984, 1994, 2004, 2014, and 2023 are shown in Figures 3, 4, 5, 6, 7, and 8. These images demonstrate that the sample points were chosen appropriately by showing how ground objects' spectral properties of reflection in the flow domain match those of typical ground objects.

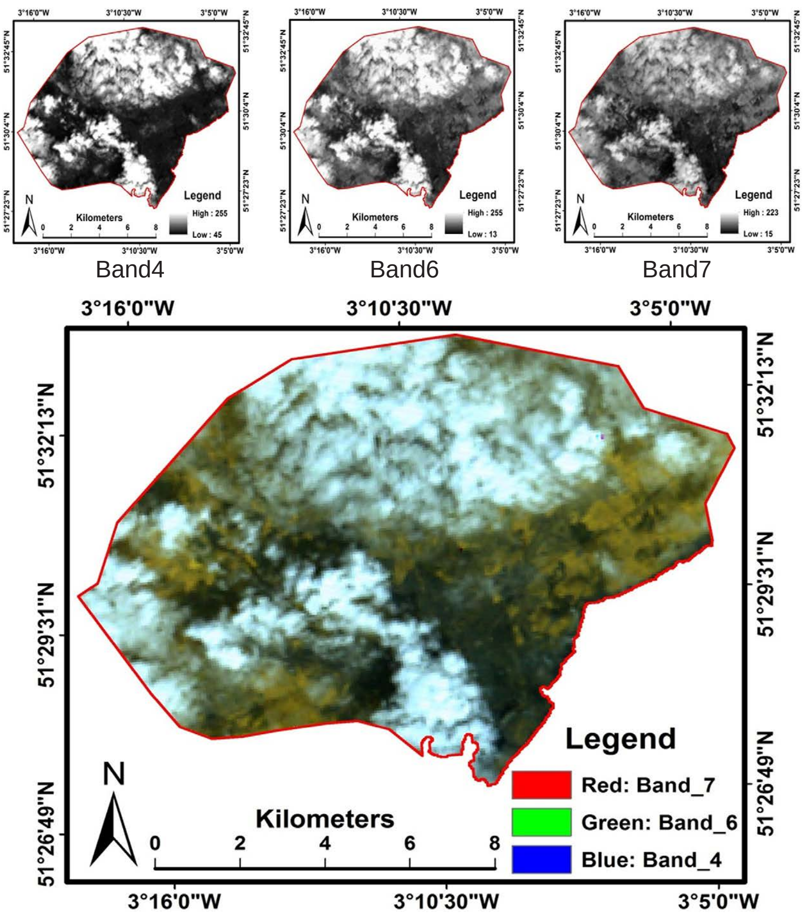

Figure 3. Composite Band of Landsat MSS of Cardiff City for year 1974

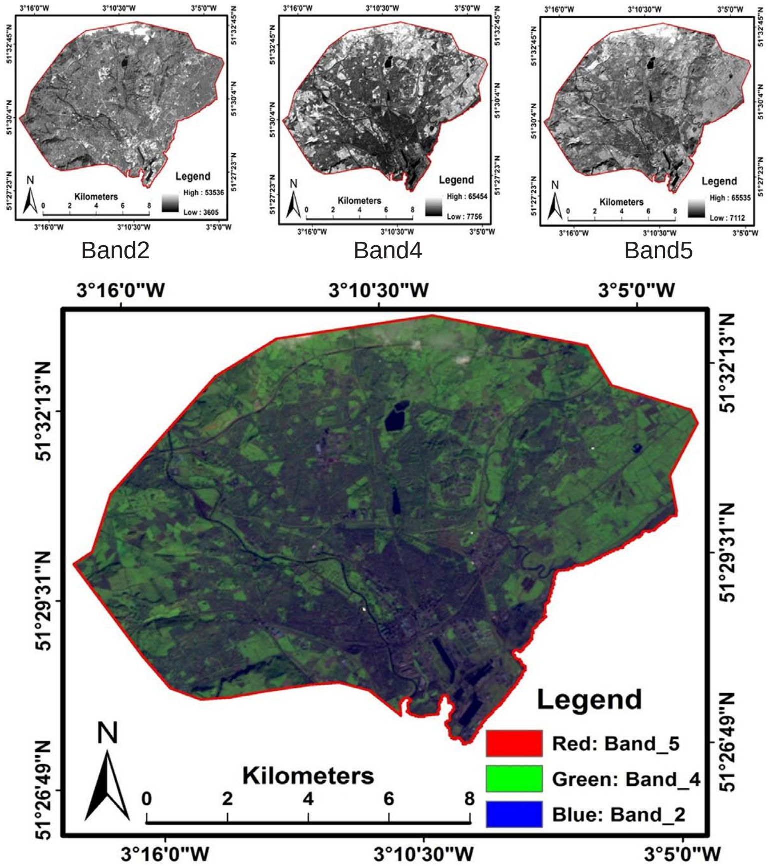

Figure 4. Composite Band of Landsat TM of Cardiff City for year 1984

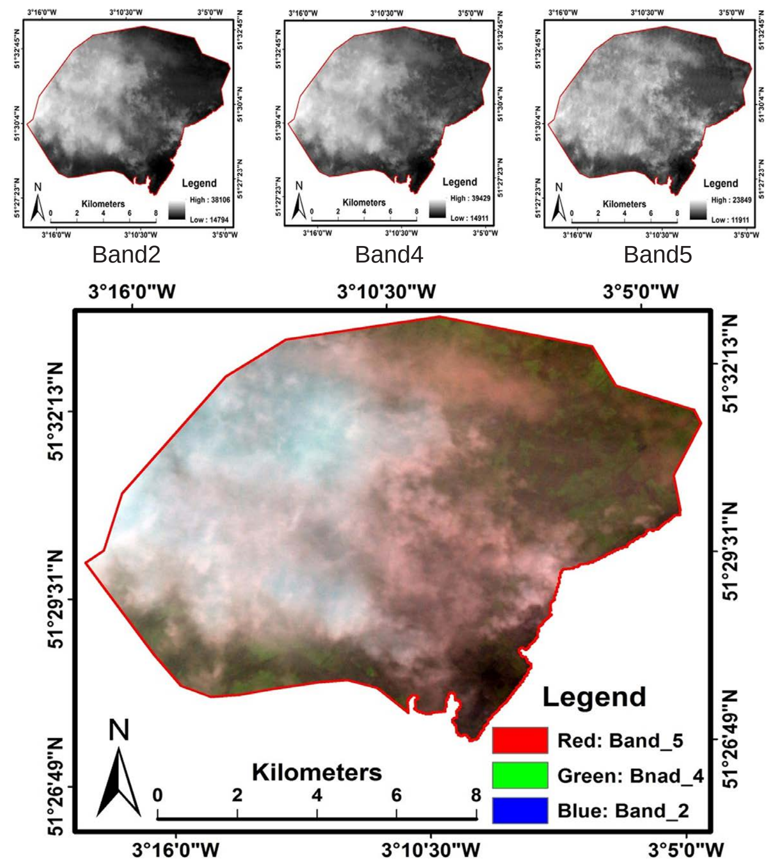

Figure 5. Composite Band of Landsat TM of Cardiff City for year 1994

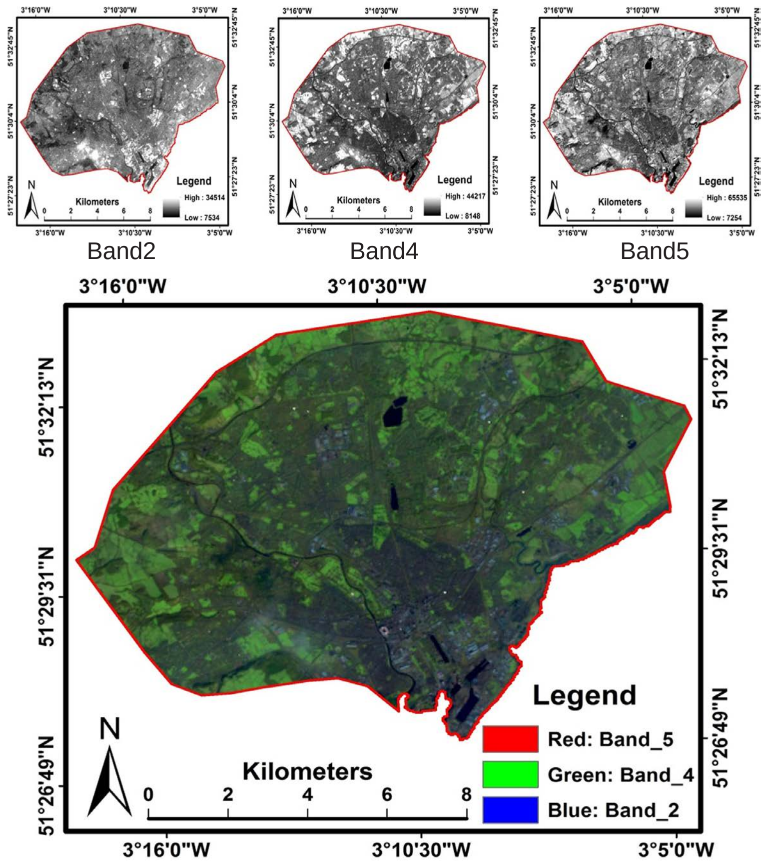

Figure 6. Composite Band of Landsat TM of Cardiff City for year 2004

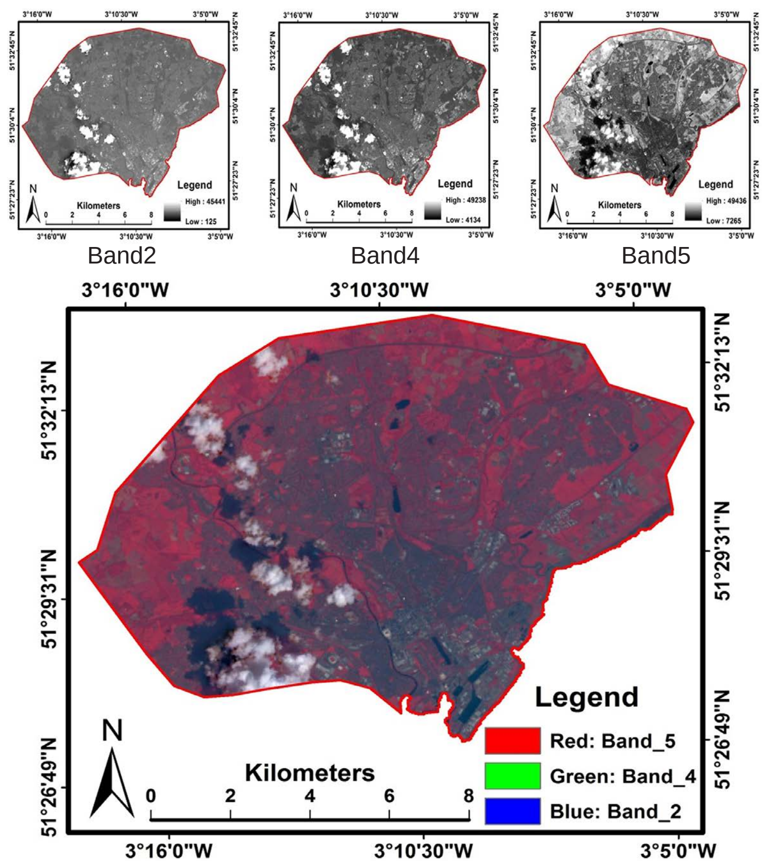

Figure 7. Composite Band of Landsat ETM+ of Cardiff City for year 2014

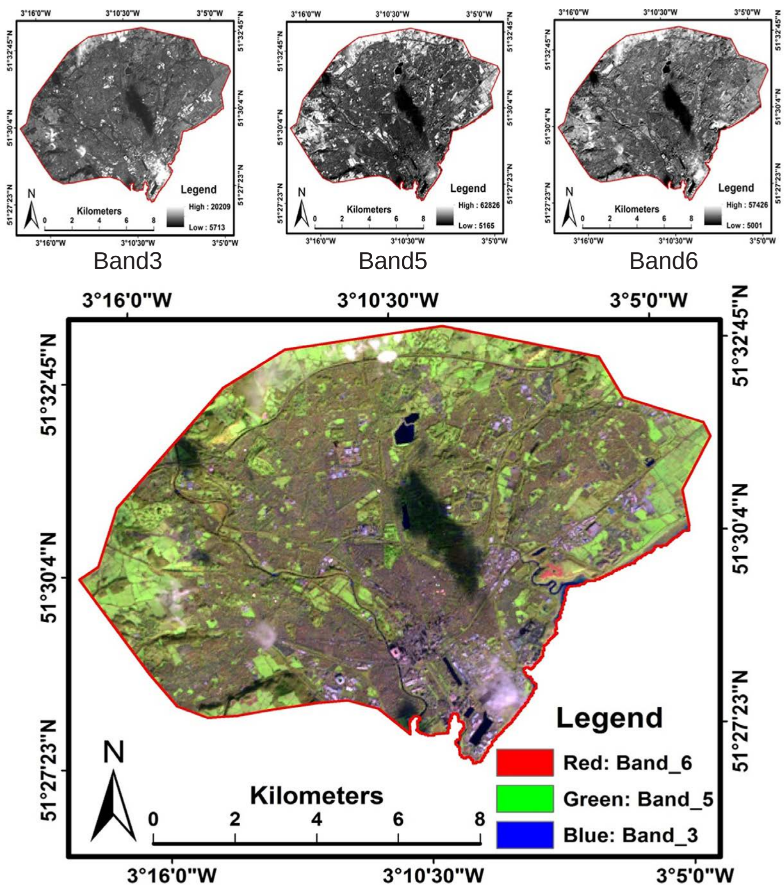

Figure 8. Composite Band of Landsat 8 OLI of Cardiff City for year 2023

RESULTS ANALYSIS

Water is recognized as crucial all around the world. Both human survival and environmental requirements depend on it. However, variations in size and density of surface water resources are possible due to human and climatic effects. The benefit of the satellite remote sensing images-based surface water extraction technique is the speed with which it can collect surface water data. When applied to extract surface water information in big, complicated geographic regions and lengthy data sets, however, a substantial number of pixel misidentification and extensive image preparation labor are inevitable. The exact management of water resources and ecological restoration in Cardiff City rely heavily on timely acquisition of correct pixel water surface percentage information using remote sensing. Enhanced Water Index (EWI) is a straightforward model developed in response to the fact that most existing water information models fail to adequately extract pixels that include information about the percentage of water surface. The EWI will be transformed from numerical values to maps showing just the locations of surface water bodies (SWBs) and dry land (NO-SWBs).

To detect the SW area changes in Cardiff City in the years 1974, 1984, 1994, 2004, 2014, and 2023, the EWI is used to glean hydrological elements. The extracted SWBs are highly affected by climate change over the time series which in turns depending upon the actions of the weather activities. As a result, we were able to gauge how efficient EWI in extracting surface water from Landsat imagery. GIS is used to compute the EWI and the resulting WS areas of each of the selected Landsat. The index algorithm of EWI is entered into the raster calculator and executed to generate the value of the EWI. The next step is deciding on a cutoff and running the algorithm to separate wet from dry regions. The downloaded raster images are converted from that composite state into the classifies state to identify that regions collected water from the others without water. After an EWI is generated and water features selected and saved., the images have been converted by the reclassifying unit to show only two regions, one with water (SWB) and one without water (NO-SWB) as it can be seen in Figure 9.

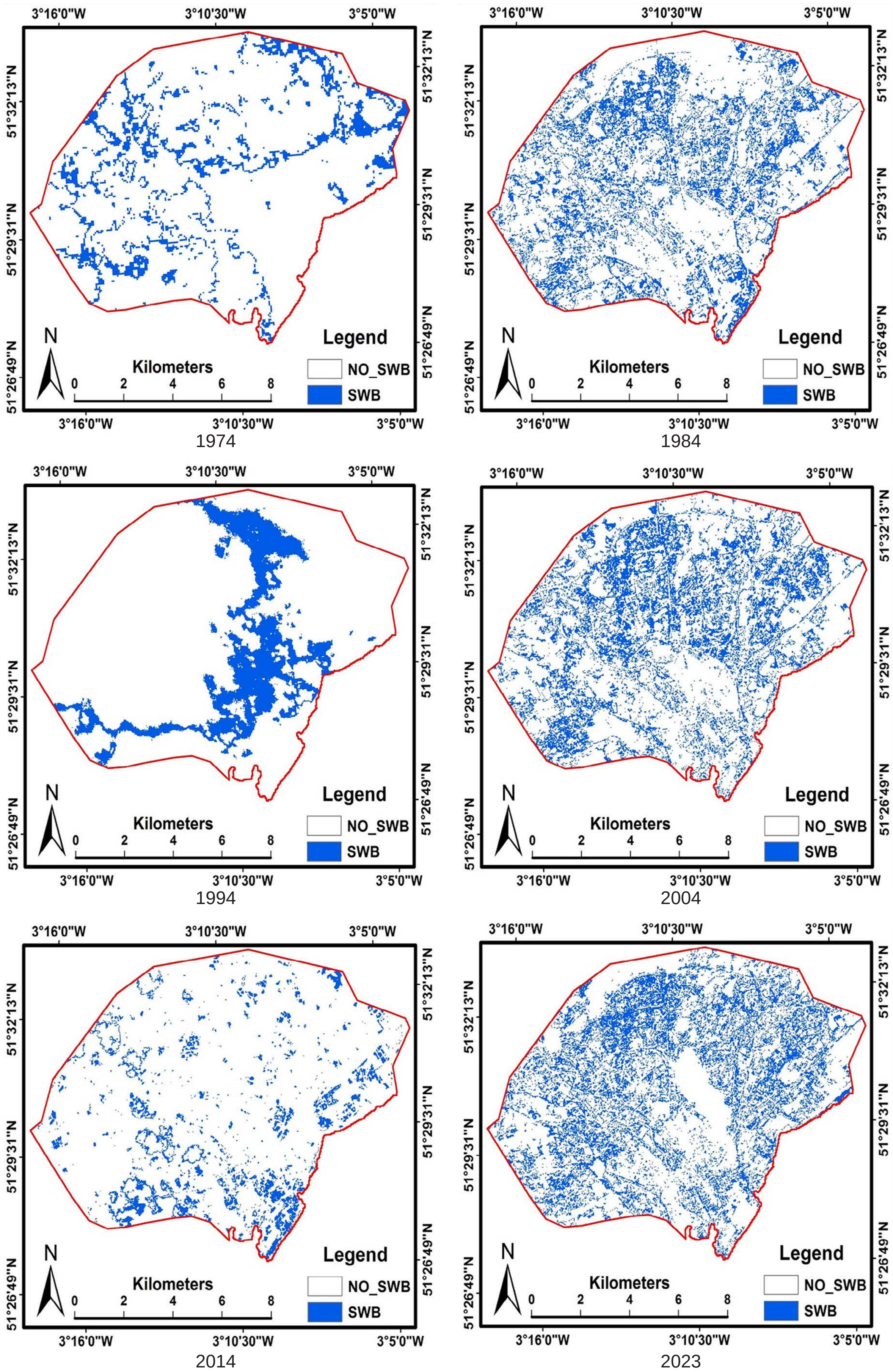

Figure 9. Extracted surface water bodies (SWB) of Cardiff City for the years 1974, 1984, 1994, 2004, 2014, and 2023

By analyzing figure 9, we make notice of the fact that the water regions that are retrieved in 1974 using the MSS Landsat pictures were few and not dense. This is due to the low levels of precipitation that occurred during that year. The distribution of water in this manner may not have a significant impact on the soil moisture, which may make it arable. The relative humidity that the soil contains is low, which prevents the soil from becoming muddy as a result of the water's presence. Changes in climate and global warming, which first became visible on the surface and began to have an effect on a variety of terrestrial activities, started to play a significant role in manipulating the amounts of rain (by either increasing or decreasing it), with temperatures that seemed to increase dramatically, which predicts the risk of an increase in evaporation rates that is unprecedented. Where we note that in the year 1984, the regions of extracted water are very vast and wide when compared to the preceding ten years, as the rates of rain can be clearly observed by rising volumes, through the analysis of images of Landsat TM. This is where we note that in the year 1984, the areas of extracted water were very large and wide. Although the amount of rain that falls may have a beneficial effect by increasing the land areas that contain water, the fact that these large land areas contain water may have an impact on the increase in the relative humidity of the soil, in addition to the high rates of groundwater that may affect the growth of plants and therefore have an impact on plant wealth, is a potential downside. In the year 1994, and by examining the images of Landsat TM, we noticed that the extreme climatic influence has a big impact on the extracted water areas, as it receded greatly in the study area, as a result of the enormous and rapid decline in the amounts of rain that had been falling. This is due to the fact that the amount of rain that had been falling had significantly decreased. The large range of climatic changes leads as a result to the unpredictability of future events that may have a significant impact or less intensity, resulting to a scarcity of some critical resources that are required by humans. Analysis conducted by Landsat TM for the year 2004 revealed a considerable rise in the amount of land that had water removed from it in comparison to land that did not contain water and land that had been analyzed in earlier years. Where the extracted water areas are huge and widespread, and this, if anything, suggests the extent of the unforeseen climatic variations, which have taken a severe toll on the climate of the entire planet. In 2014, ETM+ Landsat photos are evaluated, and it is found that the amount of water that could be recovered from the images is limited. This is due to the fact that water areas are susceptible to changes in climate. In this section, we would like to show, as can be seen from Figure 9, that despite there being a lack of water areas, they are spread to cover all areas of the study area. This is in contrast to the areas that were extracted in 1994, when there were only a few water areas and they were not widespread, leaving some areas of the study area to suffer from drought due to the lack of available water spaces in it. The Landsat 8 OLI satellite image is examined in the year 2023, and when compared to the results of the analysis in 2014, we found that the amount of extracted water regions had significantly increased. The large amounts of rain that fell on the study area through the past months and the significant climate change that began to affect temperatures that increased in some parts of the world and decreased in other parts caused an impact on the availability of sunlight, which can lessen the effect of unwanted water spaces by increasing evaporation rates.

CONCLUSIONS

Research into water mapping has consistently centered on developing a quick and easy to use remote sensing mapping approach that provides reliable data about water. Although methods and approaches for identifying water-related information at the pixel level are mature and have commonly implemented, the high precision extracted data that covering accurate information is particularly important when floods are expected to happen in those seasons that have an extreme deficiency in water resources.

In order to rapidly and precisely map the water content over the study region, the EWI is created for this research. Cardiff city in Wales, United Kingdom has been analyzed using Landsat satellite pictures for the years 1974, 1984, 1994, 2004, 2014, and 2023 to look at the distribution of surface water bodies. Extracting the EWI data and converting them to wet and dry zones has been made easier with the help of a GIS. Water in Cardiff must be directed into the nearest river with greater accuracy due to the city's high population density. The SWB zones of the huge areas are isolated with time, forming a big area in remote sensing images, and more precise spatial water surface distribution information is required for ecological environment and water resources precision management. Where water scarcity was an issue for SWBs in 1974, 1994, and 2014, resulting in significant areas being left without any SWBs. At this time, it is possible to estimate that the climate effect will repeat itself every 20 years. While in 1984, 2004, and 2023, large areas were covered by SWBs, which could have an impact on the soil and the biodiversity of the studied area. The analysis performed throughout this study demonstrates that the EWI model is credible in the context of this investigation. Temperatures have been seen to rise steadily since the year 1994, with a noticeable spike attributable to global warming. Wet and dry years have less of an effect on seasonal water than permanent water, as shown by the inter-annual change in water bodies and elevation. Expression value utilized to extract the EWI demonstrates that the EWI model provides a transparent presentation of the water content and accurate prediction of the water content fractions.

REFERENCES

1. Acharya, T.D., Subedi, A., Huang, H., Lee, D.H. 2019. Application of water indices in surface water change detection using Landsat imagery in Nepal. Sens. Mater., 31, 1429–1447.
2. Alam, A., Bhat, M.S., Maheen, M. 2020. Using Landsat satellite data for assessing the land use and land cover change in Kashmir valley. GeoJournal, 85(6), 1529–1543.
3. Allen, G.H., Pavelsky, T.M. 2018. Global extent of rivers and streams. Science, 361, 585–588.
4. Aznarez, C., Jimeno-Sáez, P., López-Ballesteros, A., Pacheco, J. P., Senent-Aparicio, J. 2021. Analysing the impact of climate change on hydrological ecosystem services in Laguna del Sauce (Uruguay) using the SWAT model and remote sensing data. Remote Sens., 13, 2014.
5. Bretreger, D., Yeo, I.-Y., Kuczera, G., Hancock, G. 2021. Remote sensing's role in improving transboundary water regulation and compliance: The Murray-Darling Basin. Australia. J. Hydrol., 13, 100–112.
6. Cao, H.Y., Han, L., Liu, Z.H., Li, L.Z. 2021. Monitoring and driving force analysis of spatial and temporal change of water area of Hongjiannao Lake from 1973 to 2019. Ecol. Inform., 61, 101230.
7. Cardiff Boasts Record Visitor Numbers During (2017). Business News Wales. 26 March 2018. Archived from the original on 7 July 2018. [Accessed: 30 June 2023].
8. Chen, J., Mueller, V. 2018. Coastal climate change, soil salinity and human migration in Bangladesh. Nat. Clim. Chang., 8, 981–985.
9. Colditz, R.R., Troche Souza, C., Vazquez, B., Wickel, A.J., Ressl, R. 2018. Analysis of optimal thresholds for identification of open water using MODIS-derived spectral indices for two coastal wetland systems in Mexico. Int. J. Appl. Earth Obs. Geoinf., 70, 13–24.
10. Danaher, T., Collett, L. 2006. Development, optimization and multi-temporal application of a simple Landsat based water index. In Proceedings of the 13th Australasian Remote Sensing and Photogrammetry Conference, Canberra, ACT, Australia, 20–24 November.
11. Domeneghetti, A. Schumann, G.J.P., Tarpanelli, A. 2019. Preface: Remote sensing for flood mapping and monitoring of flood dynamics. Remote Sens., 11, 943.
12. Feyisa, G.L., Meilby, H., Fensholt, R., Proud, S.R. 2014. AutomatedWater Extraction Index: A new technique for surface water mapping using Landsat imagery. Remote Sens. Environ., 140, 23–35.
13. Garrido-Rubio, J., Calera, A., Arellano, I., Belmonte, M., Fraile, L., Ortega, T., Bravo, R., González-Piqueras, J. 2020. Evaluation of remote sensing-based irrigation water accounting at river basin district management scale. Remote Sens., 12, 3187.
14. Iowerth, D. 1998. Castell Morgraig. Castle Studies Group Newsletter. Archived from the original on 7 September 2008. [Accessed: 30 June 2023].
15. Lu, Z., Wang, D.Q., Deng, Z.D., Shi, Y., Ding, Z.B., Ning, H., Zhao, H.F., Zhao, J.Z., Xu, H.L., Zhao, X. N. 2021. Application of red edge band in remote sensing extraction of surface water body: A case study based on GF-6 WFV data in arid area. Hydrol. Res., 52, 1526–1541.
16. Malahlela, O.E. 2016. Inland waterbody mapping: Towards improving discrimination and extraction of inland surface water features. Int. J. Remote Sens., 2016, 37, 4574–4589.
17. McFeeters, S.K. 1996. The use of the Normalized Difference Water Index (NDWI) in the delineation of open water features. Int. J. Remote Sens., 17, 1425–1432.
18. Met Office: averages 1971–2000. Met Office website (2009). Met Office. 2009. Archived from the original on 29 September 2007. [Accessed: 30 June 2023].
19. Müller, M.F., Yoon, J., Gorelick, S.M., Avisse, N., Tilmant, A. 2016. Impact of the Syrian refugee crisis

on land use and transboundary freshwater resources. Proc. Natl. Acad. Sci., 113, 14932–14937.

20. Ogilvie, A., Belaud, G., Massuel, S., Mulligan, M., Le Goulven, P., Calvez, R. 2018. Surface water monitoring in small water bodies: Potential and limits of multi-sensor Landsat time series. Hydrol. Earth Syst. Sci., 22, 4349–4380.
21. Papa, F., Crétaux, J.F., Grippa, M., Robert, E., Trigg, M., Tshimanga, R.M., Kitambo, B., Paris, A., Carr, A., Fleischmann, A.S. 2022. Water resources in Africa under global change: Monitoring surface waters from space. Surv. Geophys., 20, 1–51.
22. Parente, L., Mesquita, V., Miziara, F., Baumann, L., Ferreira, L. (2019). Assessing the Pasturelands and Livestock Dynamics in Brazil from 1985 to 2017: A Novel Approach Based on High Spatial Resolution Imagery and Google Earth Engine Cloud Computing. Remote Sens. Environ., 232, 111301.
23. Radley, J.D., Twitchett, R.J., Mander, L., Cope, J.C.W. 2008. Discussion on palaeoecology of the Late Triassic extinction event in the SW UK". Journal of the Geological Society. Geological Society of London, 165(5), 988–992.
24. Somasundaram, D., Zhang, F., Ediriweera, S., Wang, S., Li, J., Zhang, B. 2020. Spatial and Temporal Changes in Surface Water Area of Sri Lanka over a 30-Year Period. Remote Sens., 12, 3701.
25. Tariq, A., Shu, H., Kuriqi, A., Siddiqui, S., Gagnon, A.S., Lu, L.L., Linh, N.T.T., Pham, Q.B. 2021. Characterization of the 2014 Indus River Flood Using Hydraulic Simulations and Satellite Images. Remote Sens., 13, 2053.
26. UK Census. 2011. Local Area Report – Cardiff Local Authority (1946157397). Nomis. Office for National Statistics. [Accessed: 30 June 2023].
27. Vinayaraj, P., Imamoglu, N., Nakamura, R., Oda, A. 2018. Investigation on perceptron learning for water region estimation using large-scale multispectral images. Sensors, 18, 4333.
28. Weather at Cardiff Airport (CWL): Weather and Climate in Cardiff Area, Wales, (2009). U. Airports guides website. TravelSmart Ltd. 2009. Archived from the original on 14 September 2009. [Accessed: 30 June 2023].
29. Yamazaki, D., Trigg, M.A., Ikeshima, D. 2015. Development of a global similar to 90 m water body map using multi-temporal Landsat images. Remote Sens. Environ., 171, 337–351.
30. Yan, P., Zhang, Y., Zhang, Y. 2007. A study on information extraction of water enhanced water index (EWI) and GIS system in semi-arid regions with the based noise remove techniques. Remote Sens. Inf., 6, 62–67.
31. Yang, Y., Ruan, R.Z. 2010. Extraction of Plain Lake-Water Body Based on TM Imagery. Remote Sens. Inf., 3, 60–64.
32. Zhang, Q., Wu, B., Yang, Y.K. 2018. Extraction of Open Water in Rugged Area with A Novel Slope Adjusted Water Index. Remote Sens. Inf., 33, 98–107.
33. Zou, Z.H., Xiao, X.M., Dong, J.W., Qin, Y.W., Doughty, R.B., Menarguez, M.A., Zhang, G., Wang, J. 2016. Divergent trends of open surface water body area in the contiguous United States from 1984 to 2016. Proc. Natl. Acad. Sci., 115, 3810–3815.